This is the accepted manuscript (postprint) of the following article:
N. Negahdari, M. Alizadeh, S. Pashangeh, E. Salahinejad, *Structure and corrosion behavior of Cu-26Zn-5Al alloy processed by accumulative roll bonding and heat treatment*, Journal of Alloys and Compounds, 924 (2022) 166574.
https://doi.org/10.1016/j.jallcom.2022.166574

Structure and corrosion behavior of Cu-26Zn-5Al alloy processed by accumulative roll bonding and heat treatment

Nikzad Negahdari [a], Morteza Alizadeh [a,1], Shima Pashangeh [a], Erfan Salahinejad [b]

[a] *Department of Materials Science and Engineering, Shiraz University of Technology, Modarres Blvd., 71557-13876 Shiraz, Iran*

[b] *Faculty of Materials Science and Engineering, K.N. Toosi University of Technology, Tehran, Iran*

Abstract

Cu-26Zn-5Al shape memory alloy (SMA) was produced by accumulative roll bonding (ARB) and subsequent heat treatment. In this regard, different austenitization cycles and cooling conditions, including furnace, air, cold-water, and boiling-water cooling were experimented. The heat-treated specimens were characterized by scanning electron microscopy (SEM), differential scanning calorimetry (DSC), and X-ray diffraction (XRD). The corrosion behavior of the specimens was also studied by potentiodynamic polarization and electrochemical impedance spectroscopy (EIS) in a 3.5 wt% NaCl solution. The results revealed that only by cooling in the boiling- and ice-water environments, a fully martensitic microstructure showing the shape memory effect is obtained. In contrast, by using the other cooling conditions, different phases like α-phase (Cu-saturated solid solution) are formed as well as martensite. From the corrosion testing results, it was found that the SMA specimens with the fully martensitic microstructure have the highest corrosion resistance, where cooling in boiling water was recognized to be optimal. In conclusion, Cu-26Zn-5Al SMA with an

[1] Corresponding author. *E-mail address:* Alizadeh@sutech.ac.ir (M. Alizadeh).

This is the accepted manuscript (postprint) of the following article:
N. Negahdari, M. Alizadeh, S. Pashangeh, E. Salahinejad, *Structure and corrosion behavior of Cu-26Zn-5Al alloy processed by accumulative roll bonding and heat treatment*, Journal of Alloys and Compounds, 924 (2022) 166574.
https://doi.org/10.1016/j.jallcom.2022.166574

improved corrosion resistance can be produced by ARB followed by controlled heat treatment.

Keywords: Shape memory alloy (SMA); Accumulative roll bonding (ARB); Corrosion behavior; Heat treatment; Martensite

1. Introduction

Shape memory alloys (SMAs) of the ternary Cu−Al−Zn system have been developed for different applications, such as sensing, medical, automotive, and aerospace industries, due to their excellent properties like the shape memory effects [1,2]. These advanced materials show a reversible transformation from austenite to martensite without recrystallization. That is, SMAs can both present a superelastic behavior and a level of plastic deformation followed by recovery to their original shape by a thermally activated solid-state transformation. Ni-Ti [3], Fe-based (such as Fe-Pd, Fe-Pt) [4], Au- based (Au-Cu and Au-Cd) [5], and Cu-based (Cu-Zn-Al) [6] alloys have been identified as the most attractive groups of SMAs. Among them, Ni-Ti SMAs have costly processing, but Cu-based SMAs have an acceptable shape memory effect with a more economical cost [7].

Cu–Zn–Al alloys in Cu-based SMA systems are the most significant group developed for different applications, such as fasteners, couplings, and thermal actuators, where the application of other SMAs is economically and technically ineffective [8,9]. The alloying elements of Cu-Zn-Al SMAs can be altered in a wide range of contents, for example, 15–30 and 3–7 wt% for Zn and Al, respectively [10]. The initial structure of Cu-Zn-Al SMAs is the body-centered cubic (BCC) high-temperature austenite phase (β) which is transformed into the cubic close packing (CCP) low-temperature martensite phase (β′) [11]. However, the

This is the accepted manuscript (postprint) of the following article:
N. Negahdari, M. Alizadeh, S. Pashangeh, E. Salahinejad, *Structure and corrosion behavior of Cu-26Zn-5Al alloy processed by accumulative roll bonding and heat treatment*, Journal of Alloys and Compounds, 924 (2022) 166574.
https://doi.org/10.1016/j.jallcom.2022.166574

austenite phase is the only phase that exhibits the shape memory effect of practical importance. So, Cu-Zn-Al alloys are usually quenched to achieve the austenite phase for further transformation to martensite.

Different methods like casting and powder metallurgy have been used for fabricating Cu-based SMAs [7,12]. These fabrication methods have different limitations, such as the need for vacuum or shielding gases to prevent the oxidation and evaporation of alloying elements during casting methods or the formation of defects during compaction and sintering in powder metallurgy processes [13,14]. The accumulative roll bonding (ARB) process combined with a suitable heat treatment process has been used as a new method for the fabrication of Cu-Al-Mn and Cu-Zn-Al SMAs [15]. This fabrication process has different advantages, such as producing in the form of sheets with the ultrafine-grained structure without using additive alloying elements like B, Ti, V, Cr, and Zr [16].

Up to now, the structural, shape memory, and mechanical properties of Cu-Zn-Al SMAs have been extensively investigated [6,17,18]. Cu–Zn–Al alloys show a relatively higher strain recovery compared to other Cu-based alloys. However, similar to other Cu- based alloys, Cu–Zn–Al alloys reveal low fracture and fatigue strengths [12]. Si et al. [19] showed that the damping capacity of Cu- Zn-Al alloy with about 26 wt% Zn is higher than the Zn-free alloy. However, the corrosion properties of this group of SMAs have received less attention. Among limited research works conducted, De Filippo et al. [20] revealed that the electrochemical corrosion of Cu- based SMAs in the marine environment has no significant effect on their shape memory effect. However, there is still a research gap on the corrosion behavior of Cu-Zn-Al SMAs. In the present work, Cu- 26Zn-5Al SMA was produced by the ARB process combined with heat treatment at various temperatures, times and cooling

This is the accepted manuscript (postprint) of the following article:
N. Negahdari, M. Alizadeh, S. Pashangeh, E. Salahinejad, *Structure and corrosion behavior of Cu-26Zn-5Al alloy processed by accumulative roll bonding and heat treatment*, Journal of Alloys and Compounds, 924 (2022) 166574.
https://doi.org/10.1016/j.jallcom.2022.166574

conditions. The microstructural and corrosion behaviors of the fabricated alloys were studied in detail, whereas their shape memory effects have been assessed elsewhere [21].

2. Experimental procedure

2.1. Specimen preparation

In this research, commercially pure Cu, Zn, and Al sheets (Aluminum rolling company, Iran) with characteristics listed in Table 1 were used for the composite fabrication.

Table 1. Characteristics of the Cu, Zn, Al sheets used for the composite fabrication.

Raw material	Purity (%)	Dimension (mm^2)	Thickness (mm)	Tensile strength (MPa)	Elongation (%)
Cu	99.9	200 × 100	0.7	232	48
Zn	99.2	200 × 100	0.5	167	18
Al	99.8	200 × 100	0.2	70	39

In the first step, multilayered Cu/Zn/Al composite specimens were produced by the ARB process. For this purpose, three Cu, two Zn, and two Al sheets (with the sequence of Cu/Zn/Al/Cu/Zn/Al/Cu) were put on each other after surface preparation, including surface cleaning with acetone and wire brushing. The prepared sandwiches were roll-bonded by using a rolling machine of 30-ton capacity, 20 cm rolls diameter, and rolling speed of 10 rpm (Sepahan 84 D, Iran) at room temperature with 66 % reduction in thickness to make good bonding between the sheets. Then, the roll-bonded sheet was cut into two pieces, surface

This is the accepted manuscript (postprint) of the following article:
N. Negahdari, M. Alizadeh, S. Pashangeh, E. Salahinejad, *Structure and corrosion behavior of Cu-26Zn-5Al alloy processed by accumulative roll bonding and heat treatment*, Journal of Alloys and Compounds, 924 (2022) 166574.
https://doi.org/10.1016/j.jallcom.2022.166574

preparation was done on them, and they were put on each other and roll-bonded with 50 % reduction. The ARB process was done up to 9 cycles for achieving a relatively uniform microstructure in the multilayered composite specimens. Details of the ARB procedure have been discussed in Ref. [22].

In the second step, Cu-26Zn-5Al SMAs were produced by performing heat treatment processes on the multilayered composite specimens after 9 cycles of the ARB process. An electrical furnace was used at different temperatures (750, 825, and 900 °C) for different holding times (15 min to 3 h) under different cooling conditions, including boiling water, ice water, air, and furnace cooling. The heat treatment temperatures were selected based on previous work [21] with the aim of obtaining a fully austenitic structure at the annealing temperature which produces a fully martensitic structure upon quenching.

2.2. Characterization techniques

The microstructure of both the multilayered Cu/Zn/Al composites and Cu-Zn-Al SMAs specimens was investigated by field emission gun scanning electron microscope (FEG-SEM, MIRA3TESCAN-XMU, Czech Republic) combined with energy dispersive X-ray spectroscopy (EDS) at the voltage of 10 keV. Microstructural details were investigated on the rolling direction-normal direction (RD-ND) plane after surface preparation and etching according to the ASTM E3–11(2017) standard.

The phase transformation of the produced SMAs specimens was examined by using differential scanning calorimetry (DSC) in the atmosphere. For this purpose, the SMA specimens processed by heat treatment at 900 ºC for 2 h with boiling water cooling were used

This is the accepted manuscript (postprint) of the following article:
N. Negahdari, M. Alizadeh, S. Pashangeh, E. Salahinejad, *Structure and corrosion behavior of Cu-26Zn-5Al alloy processed by accumulative roll bonding and heat treatment*, Journal of Alloys and Compounds, 924 (2022) 166574.
https://doi.org/10.1016/j.jallcom.2022.166574

as these conditions were recognized to be optimal. The DSC analysis was done in the temperature range of 10 ºC to 200 ºC at a heating rate of 10 ºC/min.

The phase examination was also done by X-ray diffraction (XRD, D8 Bruker Advance Diffractometer, Bruker Company, Germany) with X-ray tube Cu Kα (λ = 1.541874 Å) in the 2θ range of 30-90°. The working voltage of the diffractometer was 40 kV and the current was 40 mA. The step time was also selected to be 3 s and the step size was 0.05 °.

The electrochemical corrosion behavior of the produced Cu-Zn-Al SMAs prepared by the different heat treatment conditions was examined by a potentiostat (Vertex, Ivium, Netherlands) in a 3.5 wt % sodium chloride (NaCl) aqueous solution (pH=8.5). For this purpose, different rectangular specimens were prepared and all of their faces except the cross-section perpendicular to the rolling direction were insulated, giving the dimensions of 6 × 1 mm^2. Before corrosion tests, the prepared specimens were polished according to the ASTM G1–90 standard, the specimens were washed with water and detergent, and finally, they were degreased with acetone. A silver-silver chloride (Ag/AgCl) electrode and a platinum rod of 5 mm in diameter and 1 mm in height were selected as the reference and auxiliary electrode, respectively. Stern-Geary equation (Eq. 1) was used to determine the corrosion current density (i_{corr}) [23]:

$$i_{corr} = \frac{(b_a \times b_c) \times 1000}{(2.3 \times R_p \times (b_a + b_c))} \left(\frac{\mu A}{cm^2}\right) \quad (1)$$

where b_a and b_c are anodic and cathodic slopes, and R_p is the linear polarization resistance of the Tafel curves. It should be mentioned that the corrosion tests were done three times for the different heat treatment conditions, and average values and standard deviations were reported.

This is the accepted manuscript (postprint) of the following article:
N. Negahdari, M. Alizadeh, S. Pashangeh, E. Salahinejad, *Structure and corrosion behavior of Cu-26Zn-5Al alloy processed by accumulative roll bonding and heat treatment*, Journal of Alloys and Compounds, 924 (2022) 166574.
https://doi.org/10.1016/j.jallcom.2022.166574

3. Results and discussion

3.1. Microscopic evaluations

The typical SEM micrograph and related EDS elemental mapping (Fig. 1) of the fabricated Cu/Zn/Al composite specimen show that the microstructure includes a relatively uniform distribution of Zn and Al layers in the Cu matrix due to the thickness decrease of the different layers and their rupturing. The EDS elemental mapping also shows that the distribution of Cu, Zn, and Al elements is uniform in the microstructure after the 9^{th} cycle. The Zn and Al layers distribution in the matrix happens due to the difference in the mechanical properties of the layers in the specimen. In fact, in higher ARB cycles, because of the different flow properties of Cu, Zn, and Al, the rolling load is transferred from the matrix to the reinforcing layers, decreases spaces between them, and finally causes a multilayered microstructure with relatively low pores and defects in the cross-sectional micrograph of the composite produced by the 9 ARB cycles.

This is the accepted manuscript (postprint) of the following article:
N. Negahdari, M. Alizadeh, S. Pashangeh, E. Salahinejad, *Structure and corrosion behavior of Cu-26Zn-5Al alloy processed by accumulative roll bonding and heat treatment*, Journal of Alloys and Compounds, 924 (2022) 166574.
https://doi.org/10.1016/j.jallcom.2022.166574

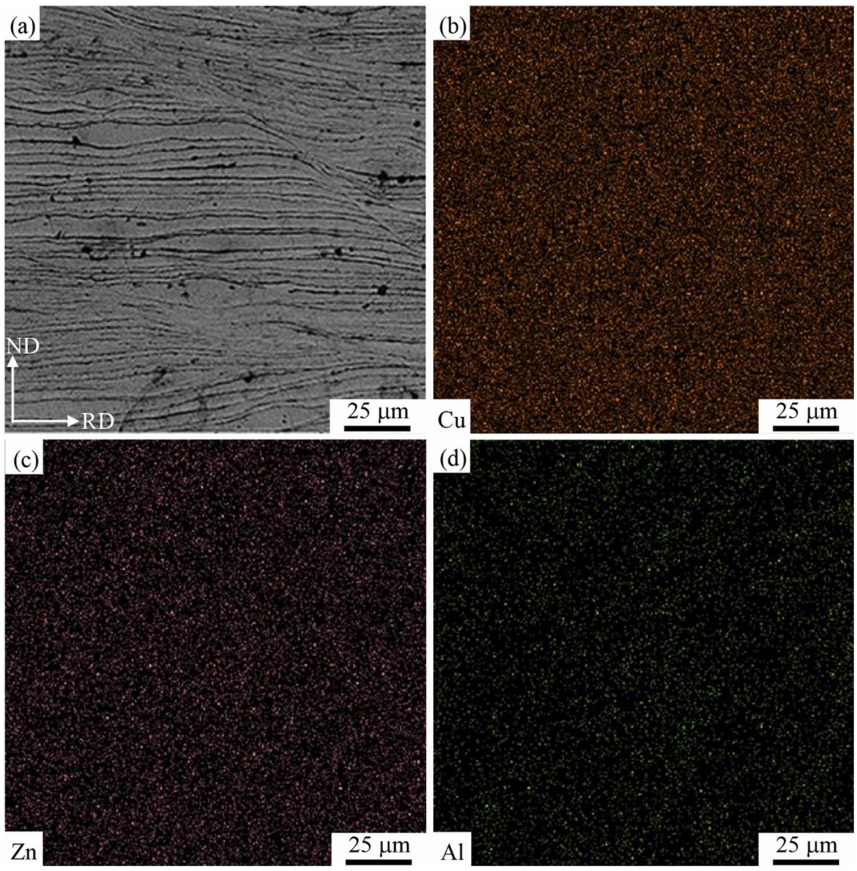

Fig. 1. SEM micrograph (a) and EDS elemental mapping related to Cu (b), Zn (c), and (d) Al in the Cu/Zn/Al composite fabricated by the 9 ARB cycles.

In the next step, the composite sample produced by the 9 ARB cycles was heat-treated to achieve the SMA alloys. Heat treatment processes were done at temperatures between 750 °C to 900 °C for different holding times between 15 min and 30 min to obtain a fully austenitic microstructure at these temperatures, followed by boiling-water cooling. Typical micrographs after the different heat treatment processes are presented in Fig. 2. The comparison of the micrographs indicates that after treatment at 750 (Figs. 2a and 2b) and 825 °C (Figs. 2c and 2d), there are two different phases in the microstructures, including fcc α-phase precipitates

This is the accepted manuscript (postprint) of the following article:
N. Negahdari, M. Alizadeh, S. Pashangeh, E. Salahinejad, *Structure and corrosion behavior of Cu-26Zn-5Al alloy processed by accumulative roll bonding and heat treatment*, Journal of Alloys and Compounds, 924 (2022) 166574.
https://doi.org/10.1016/j.jallcom.2022.166574

in the matrix after relatively slow cooling. By increasing the temperature to 900 °C (Figs. 2e and 2f), a microstructure including martensite is achieved with a needle-like morphology (β'_1 martensite) with a nonhomogeneous feature. A similar martensitic microstructure has been also reported by Aldirmaz et al. [24] and Zorica et al. [25]. Another aspect of these micrographs is that at the different holding temperatures by increasing the holding time between 15 min (Figs. 2a, 2c, and 2e) to 30 min (Figs. 2b, 2d, and 2 f), only the growth of the second phases happens. According to the Cu-Zn-Al phase diagram, the second phase which appears in the micrographs of the alloy specimens after holding at 750, 825, and 900 °C is probably the Cu- saturated α-phase, whereas the matrix is the martensite phase with a needle-like shape. For further investigations, the EDS analysis was done on different points marked in Fig. 2, and the results are tabulated in Table 2. According to the EDS data (points 1), the second phase is probably α phase [21] which decreases in amount by increasing the isothermal holding temperature between 750 °C to 900 °C. In conclusion, the SEM micrographs and EDS analyses confirm that the two different parameters of heat treatment, i.e. time and temperature after the ARB process are effective to achieve a desirable alloy in the Cu-Zn-Al system.

This is the accepted manuscript (postprint) of the following article:
N. Negahdari, M. Alizadeh, S. Pashangeh, E. Salahinejad, *Structure and corrosion behavior of Cu-26Zn-5Al alloy processed by accumulative roll bonding and heat treatment*, Journal of Alloys and Compounds, 924 (2022) 166574.
https://doi.org/10.1016/j.jallcom.2022.166574

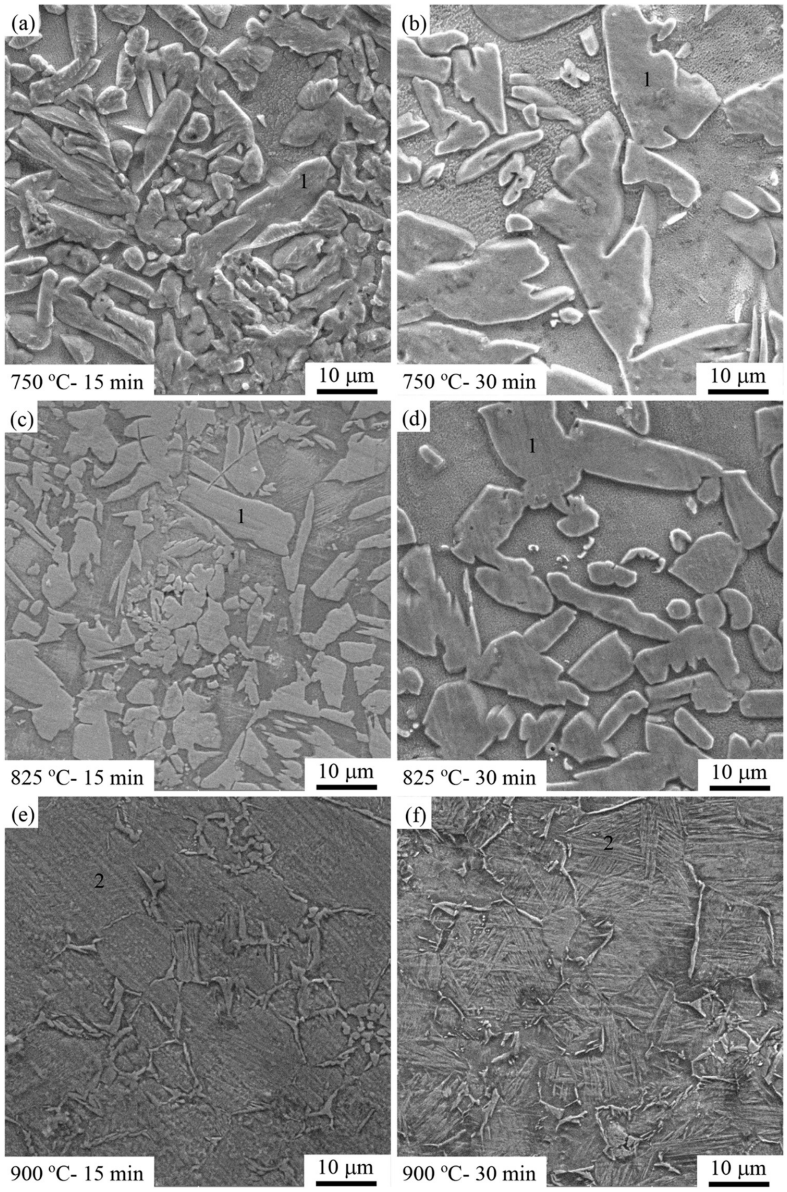

Fig. 2. SEM micrographs of the ARBed samples after heat treatment at (a and b) 750, (c and d) 825, and (e and f) 900 °C for 15 (a, c, and e) and 30 min (b, d, and f) followed by boiling water cooling. Points 1 shows α phase.

This is the accepted manuscript (postprint) of the following article:
N. Negahdari, M. Alizadeh, S. Pashangeh, E. Salahinejad, *Structure and corrosion behavior of Cu-26Zn-5Al alloy processed by accumulative roll bonding and heat treatment*, Journal of Alloys and Compounds, 924 (2022) 166574.
https://doi.org/10.1016/j.jallcom.2022.166574

Table 2. EDS results related to Regions 1 and 2 of Fig. 2.

Holding temperature (ºC)	Holding time (min)	Composition (wt.%)		
		Cu	Zn	Al
750	15	67.5	30.1	2.4
	30	69.0	28.1	2.9
825	15	68.6	29.7	2.7
	30	66.7	30.2	3.1
900	15	68.5	27.0	4.8
	30	69.0	26.0	5.0

As indicated above, the higher temperature (900 °C) was suitable for achieving a full martensitic microstructure in the Cu-26Zn-5Al alloy specimen (SMA), but holding for 15 and 30 min was not effective for the microstructure evolution towards a fully homogeneous martensitic structure in the Cu-26Zn-5Al alloy (see Figs. 2e and 2f). Thus, further isothermal holding times between 1 h and 3 h were tested at 900 °C after boiling water cooling (Fig. 3). The isothermal holding times shorter than 2 h (Figs. 3a and 3b) lead to the development of the second phase which is probably α phase, according to the EDS analysis related to Fig. 3b at Point 2 tabulated in Table 3, the phase diagram of the Cu-Zn-Al system and previous work [21]. The secondary α phase usually is mostly located at grain boundaries. According to the micrograph presented in Fig. 3c, the Cu-Zn-Al alloy after 2 h of holding at 900 °C shows a uniform martensitic microstructure (the necessary phase for SMA) and the second phase disappears. Also, according to the micrographs shown in Fig. 3, the martensite phase has a

This is the accepted manuscript (postprint) of the following article:
N. Negahdari, M. Alizadeh, S. Pashangeh, E. Salahinejad, *Structure and corrosion behavior of Cu-26Zn-5Al alloy processed by accumulative roll bonding and heat treatment*, Journal of Alloys and Compounds, 924 (2022) 166574.
https://doi.org/10.1016/j.jallcom.2022.166574

needle-like morphology characterized by colliding of different martensite plates (M18R type martensite [26]) as a typical microstructure in Cu-based alloys.

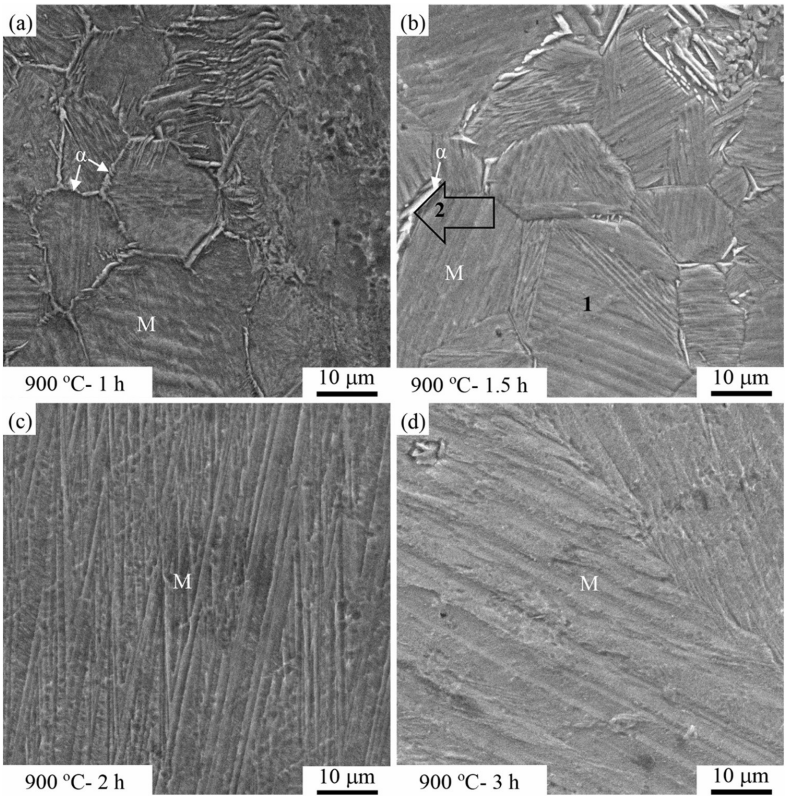

Fig. 3. SEM micrographs of the Cu-26Zn-5Al alloy after heat treatment at 900 °C for the various holding times: (a) 1, (b) 1.5, (c) 2, and (d) 3 h followed by boiling-water cooling.

Table 3. EDS results related to Subfigure 3b.

Elements	Amount (wt%)	
	Point 1	**Point 2**
Cu	68.1	73.8
Zn	26.9	22.1
Al	5.0	4.1

This is the accepted manuscript (postprint) of the following article:
N. Negahdari, M. Alizadeh, S. Pashangeh, E. Salahinejad, *Structure and corrosion behavior of Cu-26Zn-5Al alloy processed by accumulative roll bonding and heat treatment*, Journal of Alloys and Compounds, 924 (2022) 166574.
https://doi.org/10.1016/j.jallcom.2022.166574

Microstructural features after cooling in different environments, including ice-water bath, air, and furnace after 2 h of holding at 900 °C were also investigated by SEM (Fig. 4). As appears in Fig. 4a, the SMA specimen after cooling in the ice-water bath is a fully martensitic phase (which exhibits as a needle-like morphology with colliding of different martensite plates (M18R type martensite [27])) with a fine grain distribution. But by using air and furnace cooling, the final microstructure of the specimens includes two different phases, where the second phase grows more by cooling in the furnace and thereby reveals coarse grains in the final microstructure.

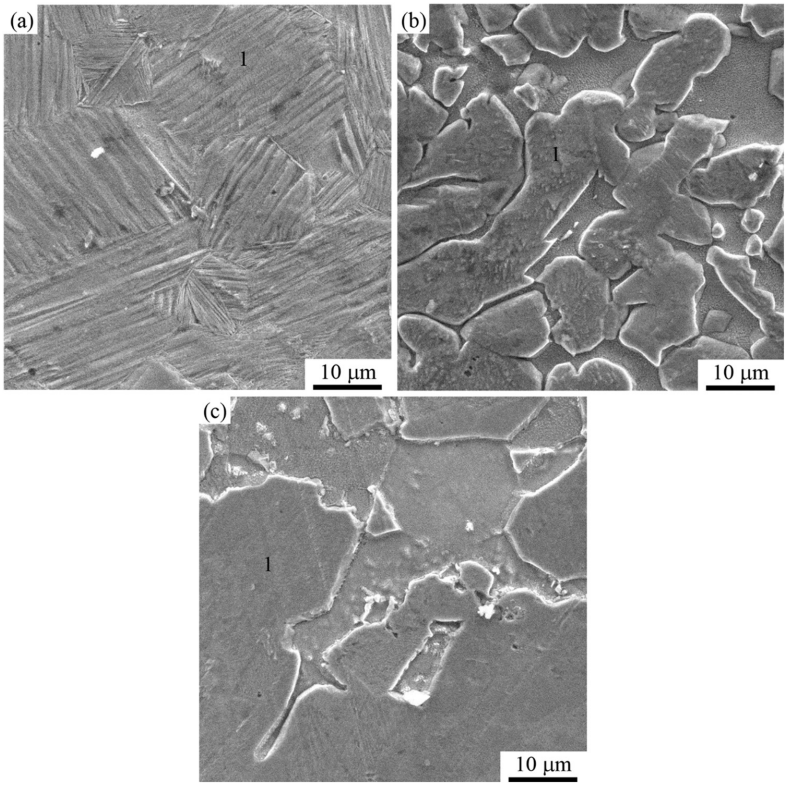

Fig. 4. SEM micrographs of the Cu-26Zn-5Al alloy after heat treatment at 900 °C and holding for 2 h followed by cooling in (a) ice water bath, (b) air cooling, and (c) furnace cooling.

This is the accepted manuscript (postprint) of the following article:
N. Negahdari, M. Alizadeh, S. Pashangeh, E. Salahinejad, *Structure and corrosion behavior of Cu-26Zn-5Al alloy processed by accumulative roll bonding and heat treatment*, Journal of Alloys and Compounds, 924 (2022) 166574.
https://doi.org/10.1016/j.jallcom.2022.166574

Also, the EDS data related to different points marked in Fig. 4 are presented in Table 4. The EDS results reveal that the second phase which appears after cooling in air and furnace is probably the α- phase. The comparison of the different cooling conditions confirms that the boiling water bath is suitable to achieve a SMA alloy in the Cu-26Zn-5Al alloy after heat treatment at 900 °C and holding for 2 h. This sample is characterized by a relatively uniform grain distribution in comparison to the other cooling conditions. Ice water cooling also showed a fully martensitic structure with a finer grains distribution in comparison to the boiling water cooling, but it may suffer from a thermal shock induced in the high cooling rate. So, boiling water cooling is introduced as the optimal condition to obtain a fully martensitic structure.

Table 4. EDS results of the Cu-Zn-Al alloy after heat treatment at 900 °C for 2 h followed by cooling in ice water, air, and furnace on Location 1 of Fig. 4.

Cooling condition	**Composition (wt.%)**		
	Cu	**Zn**	**Al**
Ice water	67.5	27.6	4.9
Air cooling	67.1	30.0	2.9
Furnace cooling	68.0	25.2	6.8

This is the accepted manuscript (postprint) of the following article:
N. Negahdari, M. Alizadeh, S. Pashangeh, E. Salahinejad, *Structure and corrosion behavior of Cu-26Zn-5Al alloy processed by accumulative roll bonding and heat treatment*, Journal of Alloys and Compounds, 924 (2022) 166574.
https://doi.org/10.1016/j.jallcom.2022.166574

3.2. Thermal studies

The DSC curve of the Cu-Zn-Al SMA heat-treated at 900 °C for 2 h followed by boiling water cooling with the martensitic structure is shown in Fig. 5. The DSC results reveal that the martensitic transformation is reversible due to peaks appearing in heating and cooling curves. Also, as can be seen in Fig. 5, during heating there is an exothermic peak that reveals the austenitic transformation. Based on the position of the transformation peaks, transformation temperatures were determined by drawing tangent lines on the peaks. The austenite start (A_s) and finish (A_f) transformation temperatures are 125 and 134 °C, respectively. During cooling, there is a peak that is related to the martensitic transformation. The martensite start (M_s) and finish (M_f) temperatures are 120 and 114 °C, respectively.

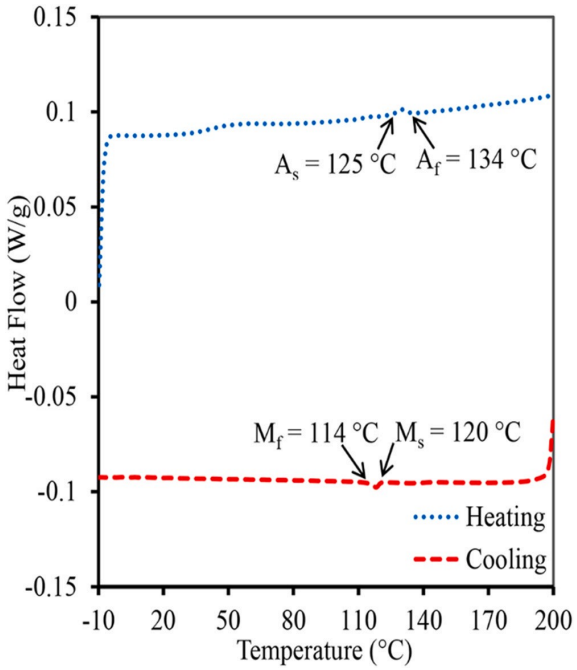

Fig. 5. DSC curve for heating and cooling of the Cu-Zn-Al SMA fabricated at 900 °C for 2 h followed by boiling water cooling.

This is the accepted manuscript (postprint) of the following article:
N. Negahdari, M. Alizadeh, S. Pashangeh, E. Salahinejad, *Structure and corrosion behavior of Cu-26Zn-5Al alloy processed by accumulative roll bonding and heat treatment*, Journal of Alloys and Compounds, 924 (2022) 166574.
https://doi.org/10.1016/j.jallcom.2022.166574

The M_s temperatures of Cu-Zn-Al alloys are typically below 200 °C [28] with a strong dependency on the chemical composition and heat treatment conditions of the alloy. The DSC analysis and critical temperatures determined suggest that achieving a fully martensitic microstructure during heat treatment is possible by boiling water bath cooling, which confirms the microstructural observations.

3.3. XRD phase investigations

The typical XRD patterns of the Cu-Zn-Al alloy specimens after heat treatment at 900 °C for 1.5 and 2 h followed by final boiling- water quenching and also for 2 h with air cooling are depicted in Fig. 6. The XRD pattern related to the air-cooling specimen shows the presence of different phases, including α (Cu-saturated solid solution), β_1, and Al_2Cu_3. However, by using boiling-water cooling after 1.5 h of isothermal annealing, different peaks related to phases, such as α, β_1, M18R, and AlCu appear in the XRD pattern. In the XRD pattern for the alloy specimen after holding at 900 °C for 2 h followed by boiling-water cooling, all peaks are related to the M18R phase (Ref. code: 00–028–0005). M18R is one of the crystalline structures of martensite with twining, which is transformed to the initial structure by heating [29,30].

This is the accepted manuscript (postprint) of the following article:
N. Negahdari, M. Alizadeh, S. Pashangeh, E. Salahinejad, *Structure and corrosion behavior of Cu-26Zn-5Al alloy processed by accumulative roll bonding and heat treatment*, Journal of Alloys and Compounds, 924 (2022) 166574.
https://doi.org/10.1016/j.jallcom.2022.166574

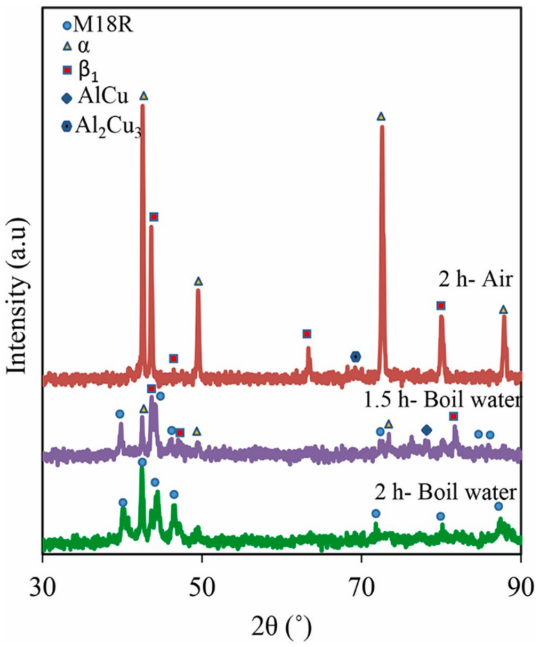

Fig. 6. XRD patterns of the Cu-Zn-Al alloy specimens after holding at 900 °C for 1.5 and 2 h followed by cooling in air and boiling water.

3.4. Corrosion behaviors

3.4.1. Comparison of the composites and alloys

Fig. 7 represents the potentiodynamic polarization curves of the Cu-Zn-Al SMA in comparison to the related Cu-Zn-Al composite produced. Overall comparing the potentiodynamic curves for both the composite and SMA specimens with a fully martensitic microstructure (cooled in boiling water) depicts that the Cu-Zn-Al SMA has a lower corrosion current density and higher corrosion potential. The corrosion current density, corrosion potential, cathodic and anodic slopes, and corrosion rate achieved from the cathodic and anodic regions of the Tafel scan by using the linear polarization resistance (Stern-Geary method) and Tafel extrapolation methods are listed in Table 5. In the composite specimen

This is the accepted manuscript (postprint) of the following article:
N. Negahdari, M. Alizadeh, S. Pashangeh, E. Salahinejad, *Structure and corrosion behavior of Cu-26Zn-5Al alloy processed by accumulative roll bonding and heat treatment*, Journal of Alloys and Compounds, 924 (2022) 166574.
https://doi.org/10.1016/j.jallcom.2022.166574

during the ARB process, residual stresses are created, which increases the internal energy and the tendency to chemical/electrochemical reactions in corroded environments [31,32]. The ARB process causes the formation of an ultrafine structure with a high density of unstable boundaries with low corrosion resistance. A previous work shows that residual strain after the ARB process affects the exchange current density during corrosion tests [32]. After the 9th ARB cycle, the Cu-Zn-Al composite specimen has a high degree of residual strain in the structure, which can provide a higher exchange current density. Also, in the composite specimens, there is a galvanic couple between the matrix and reinforcements with different corrosion tendencies. In the Cu-Zn-Al multilayered composite specimen, Zn and Al phases are more active than the Cu phase, finally causing to create a galvanic couple between the different layers during the corrosion tests and to decrease the corrosion resistance [22,33]. But in the fabricated SMA alloys in comparison to the composite specimens with the multilayered structure of the different elements, the corrosion current decreases and the corrosion potential increases to the noble value, which indicates that the corrosion tendency of the fabricated SMA is lower than that of the composite specimen. In the Cu-Zn-Al SMA after heat treatment at 900 °C for 2 h, the microstructure involves only the martensite phase without the presence of any secondary phases (Fig. 3c). So, the galvanic coupling cannot happen in the fabricated SMA specimen.

This is the accepted manuscript (postprint) of the following article:
N. Negahdari, M. Alizadeh, S. Pashangeh, E. Salahinejad, *Structure and corrosion behavior of Cu-26Zn-5Al alloy processed by accumulative roll bonding and heat treatment*, Journal of Alloys and Compounds, 924 (2022) 166574.
https://doi.org/10.1016/j.jallcom.2022.166574

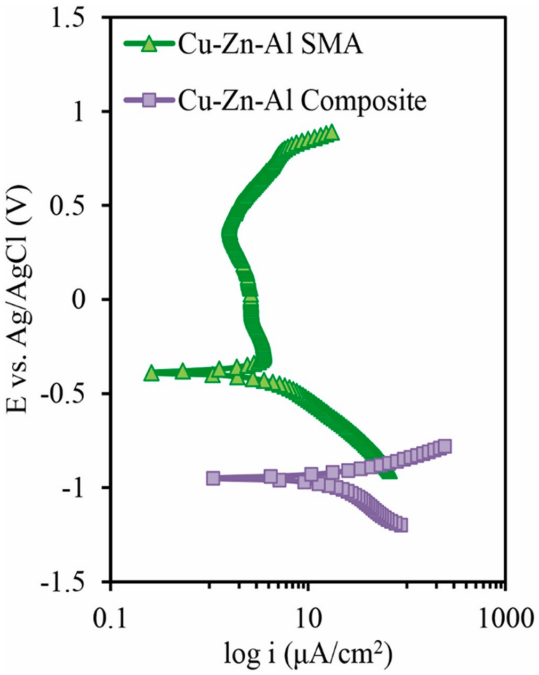

Fig. 7. Polarization curves of the Cu-Zn-Al SMA heat-treated at 900 °C for 2 h followed by boiling-water cooling and the composite specimen (after the 9th ARB cycle) on the cross-section RD-ND plane in the 3.5 wt% NaCl solution.

Table 5. Corrosion current density and corrosion potential obtained by the Tafel extrapolation and Stern-Geary methods for the Cu-Zn-Al SMA and composite specimens.

Specimen	**Tafel extrapolation method**		**Stern-Geary method**			
	i_{corr} (μA/cm^2) (±0.200)	**E_{Corr} (v) (±0.020)**	**β_a (v/dec) (±0.010)**	**β_c (v/dec) (±0.010)**	**R_p (Ω) (±50)**	**i_{corr} (μA/cm^2) (±0.200)**
SMA	1.390	-0.381	0.075	0.110	20250	**0.960**
Composite	50.118	-0.998	0.088	0.128	433	**52.360**

This is the accepted manuscript (postprint) of the following article:
N. Negahdari, M. Alizadeh, S. Pashangeh, E. Salahinejad, *Structure and corrosion behavior of Cu-26Zn-5Al alloy processed by accumulative roll bonding and heat treatment*, Journal of Alloys and Compounds, 924 (2022) 166574.
https://doi.org/10.1016/j.jallcom.2022.166574

3.4.2. Effect of cooling under different conditions for the Cu-Zn-Al alloys

To investigate the influence of the cooling conditions on the corrosion behaviors of the produced Cu-Zn-Al alloy samples, the ARBed composite specimens after holding at 900 °C for 2 h were cooled under the different conditions, including ice-water, air, furnace, and boiling water. Their potentiodynamic polarization curves in the 3.5 % NaCl solution are revealed in Fig. 8. The different corrosion parameters, including corrosion current density, corrosion potential, cathodic and anodic slopes, and corrosion rate obtained from the cathodic and anodic regions of the Tafel scan by using both the Tafel extrapolation and linear polarization resistance (Stern-Geary method) methods are tabulated in Table 6. The results show that the different cooling conditions and related structures affect the corrosion behavior. As the SEM micrographs revealed, after cooling in the furnace and air (Figs. 5b and 5c), the microstructures include the α-phase, whereas after ice-water (Fig. 5a) and boiling water (Fig. 4c) cooling, a fully martensitic microstructures are achieved. The alloy specimen cooled in the furnace has the highest corrosion current density in comparison to the other cooling conditions. Also, the noblest corrosion potential is achieved for the specimen cooled in boiling water. The higher corrosion rate of the ice-water cooled specimen in comparison to boiling water cooling is due to grain refinement, where higher cooling rates result in more grain refinement [35] and the grain refinement is one of the main parameters which affects the corrosion behavior [7,36]). In fact, a higher level of grain boundaries is obtained in the fine microstructure by using the ice-water cooling process (as seen in Fig. 5a), which act as preferred regions for corrosion. The lower corrosion resistance of the multiphasic samples (furnace and air cooling) is also attributed to microgalvanic corrosion between the different phases.

This is the accepted manuscript (postprint) of the following article:
N. Negahdari, M. Alizadeh, S. Pashangeh, E. Salahinejad, *Structure and corrosion behavior of Cu-26Zn-5Al alloy processed by accumulative roll bonding and heat treatment*, Journal of Alloys and Compounds, 924 (2022) 166574.
https://doi.org/10.1016/j.jallcom.2022.166574

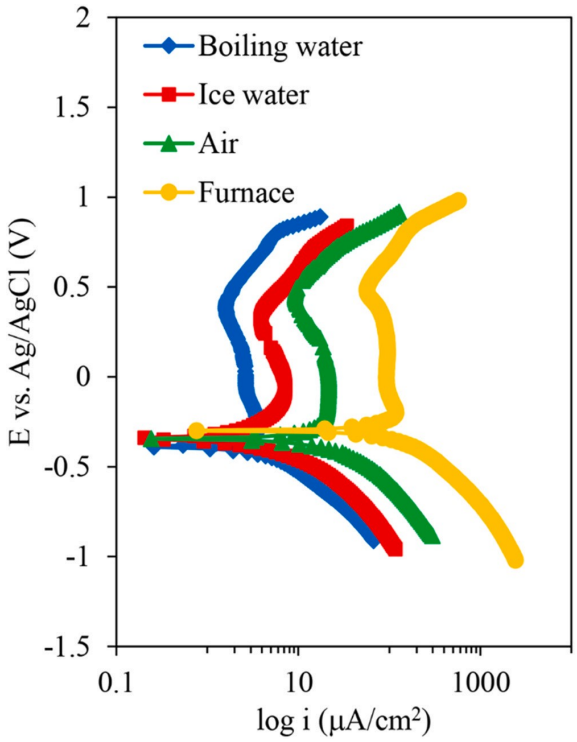

Fig. 8. Polarization curves of the Cu-Zn-Al SMA alloy specimens heat-treated at 900 °C for 2 h followed by cooling under the different cooling conditions.

Table 6. Corrosion parameters, including corrosion current density and corrosion potential achieved by the Tafel extrapolation and Stern-Geary methods for the Cu-Zn-Al alloy specimens after cooling under the different cooling conditions

Specimen	Tafel extrapolation method		Stern-Geary method			
	i_{corr} (μA/cm²) (±0.200)	E_{Corr} (v) (±0.020)	β_a (v/dec) (±0.010)	β_c (v/dec) (±0.010)	R_p (Ω) (±50)	i_{corr} (μA/cm²) (±0.200)
Boiling	1.380	-0.390	0.075	0.110	20250	**0.960**

This is the accepted manuscript (postprint) of the following article:
N. Negahdari, M. Alizadeh, S. Pashangeh, E. Salahinejad, *Structure and corrosion behavior of Cu-26Zn-5Al alloy processed by accumulative roll bonding and heat treatment*, Journal of Alloys and Compounds, 924 (2022) 166574.
https://doi.org/10.1016/j.jallcom.2022.166574

water						
Ice water	1.620	-0.345	0.085	0.115	11120	**1.911**
Air	1.746	-0.340	0.085	0.095	7980	**2.444**
Furnace	5.741	-0.299	0.115	0.096	5200	**4.401**

The electrochemical impedance spectroscopy (EIS) spectra, including Nyquist plot, total impedance Bode plot, phase angle Bode of the different alloy specimens processed under the different cooling conditions (boiling water, ice water, air, and furnace), EIS equivalent circuit model, and equivalent circuit model are also shown in Fig. 9. It is clear that the Nyquist plot of all the specimens after cooling in the different environments are similar with a single capacitance loop, indicating that a similar corrosion mechanism is dominant. The diameter of the semicircle for the SMA alloy specimen after cooling in boiling water is larger than that of the other specimens, which confirms the higher corrosion resistance of this specimen. According to Fig. 9a, the lowest corrosion resistance belongs to the specimen cooled in the furnace (the smallest loop), attributed to its multiphasic structure inducing galvanic couples. According to Fig. 9b, the alloy specimen after cooling in boiling water (the SMA specimens with the fully martensitic microstructure) has the maximum impedance (Z) value over the entire frequency range, confirming the maximum corrosion resistance in comparison to the other cooling conditions. Also, the phase angle vs. frequency curves shown in Fig. 9c appear one time constant for all the specimens in the different cooling conditions, which is in agreement with the Nyquist plots curves (Fig. 9a). The equivalent circuit shown in Fig. 9d also describes the EIS behavior of the samples, characterized by the electrolyte resistance (R_s), constant phase element of the double layer (CPE_{dl}), and charge transfer resistance (R_{ct}).

This is the accepted manuscript (postprint) of the following article:
N. Negahdari, M. Alizadeh, S. Pashangeh, E. Salahinejad, *Structure and corrosion behavior of Cu-26Zn-5Al alloy processed by accumulative roll bonding and heat treatment*, Journal of Alloys and Compounds, 924 (2022) 166574.
https://doi.org/10.1016/j.jallcom.2022.166574

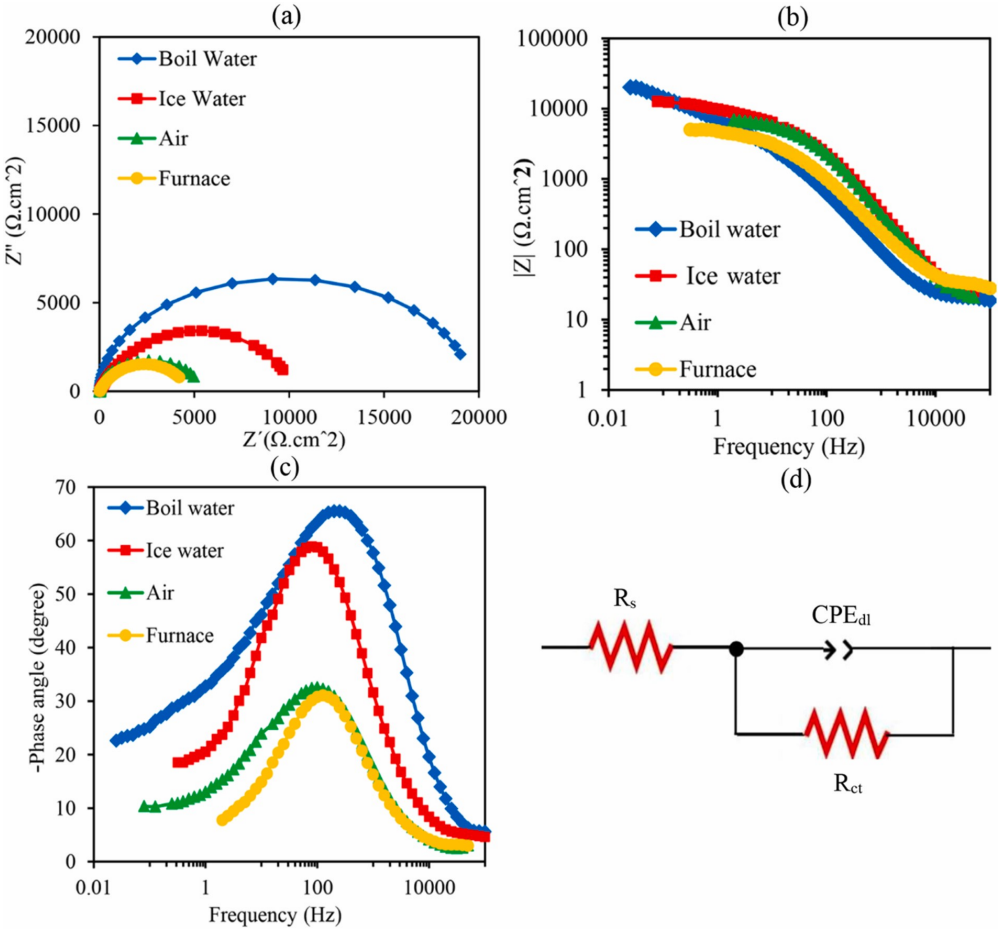

Fig. 9. (a) Nyquist, (b) total impedance Bode and (c) phase-angle Bode plots, and also (d) equivalent circuit model of the Cu-Zn-Al alloy specimens after cooling in the different environments.

4. Conclusion

This research work focused on the influence of austenitization thermal cycles and cooling conditions on the final microstructure of Cu-Zn-Al alloy and the resultant corrosion behavior in the 3.5% NaCl solution. For this purpose, ARBed Cu/Zn/Al composite specimens were

This is the accepted manuscript (postprint) of the following article:
N. Negahdari, M. Alizadeh, S. Pashangeh, E. Salahinejad, *Structure and corrosion behavior of Cu-26Zn-5Al alloy processed by accumulative roll bonding and heat treatment*, Journal of Alloys and Compounds, 924 (2022) 166574.
https://doi.org/10.1016/j.jallcom.2022.166574

heat-treated at 900 °C for 2 h and then cooled under different conditions, including boiling water, ice water, air, and furnace. The following conclusions were achieved:

1. Isothermal holding times lower than 2 h caused the presence of the α phase coupled with martensite in the final microstructure, whereas the holding time of 2 h was sufficient to achieve a fully martensite microstructure in the Cu-Zn-Al system.

2. A fully martensitic microstructure was achieved in the Cu-26Zn- 5Al alloy after 9 cycles of the ARB process combined with heat treatment at 900 °C for 2 h and cooling in boiling water and ice water. In contrast, air and furnace cooling provided multiphasic microstructures, including martensite, α, AlCu, and Al_2Cu_3.

3. The SMA alloy achieved by isothermal holding at 900 °C for 2 h and boiling water cooling with a fully martensitic microstructure showed a higher corrosion resistance in comparison to the ARBed composite specimen and the other cooling conditions.

4. The corrosion mechanism of the Cu-26Zn-5Al alloy specimens cooled under the different conditions was different. For the specimens cooled in air and furnace, multiphasic microstructures dictated microgalvanic corrosion between the different phases in contrast to the boiling and ice water cooling conditions with single-phase martensitic structures.

Data Availability

The authors do not have permission to share data. The raw data required to reproduce these findings cannot be shared at this time as the data also forms a part of an ongoing study.

This is the accepted manuscript (postprint) of the following article:
N. Negahdari, M. Alizadeh, S. Pashangeh, E. Salahinejad, *Structure and corrosion behavior of Cu-26Zn-5Al alloy processed by accumulative roll bonding and heat treatment*, Journal of Alloys and Compounds, 924 (2022) 166574.
https://doi.org/10.1016/j.jallcom.2022.166574

Declaration of Competing Interest

The authors declare that they have no known competing financial interests or personal relationships that could have appeared to influence the work reported in this paper.

References

[1] R.D. Dar, H. Yan, Y. Chen, Grain boundary engineering of Co-Ni-Al, Cu-Zn-Al, and Cu-Al-Ni shape memory alloys by intergranular precipitation of a ductile solid solution phase, Scr. Mater. 115 (2016) 113–117, https://doi.org/10.1016/j. scriptamat.2016.01.014

[2] J.M. Jani, M. Leary, A. Subic, Shape memory alloys in automotive applications, Appl. Mech. Mater. 663 (2014) 248–253.

[3] C.P. Frick, B.G. Clark, A.S. Schneider, R. Maaß, S. Van Petegem, H. Van Swygenhoven, On the plasticity of small-scale nickel-titanium shape memory alloys, Scr. Mater. 62 (2010) 492–495, https://doi.org/10.1016/j.
scriptamat.2009.12.023

[4] T. Maruyama, H. Kubo, 12 - Ferrous (Fe-based) shape memory alloys (SMAs): properties, processing and applications, in: K. Yamauchi, I. Ohkata, K. Tsuchiya, S. Miyazaki (Eds.), Shape Mem. Superelastic Alloy, Woodhead Publishing, 2011, pp. 141–159, https://doi.org/10.1533/9780857092625.2.141

[5] R. Dasgupta, A.K. Jain, P. Kumar, S. Hussein, A. Pandey, Effect of alloying constituents on the martensitic phase formation in some Cu-based SMAs, J. Mater. Res. Technol. 3 (2014) 264–273, https://doi.org/10.1016/j.jmrt.2014.06.004

This is the accepted manuscript (postprint) of the following article:
N. Negahdari, M. Alizadeh, S. Pashangeh, E. Salahinejad, *Structure and corrosion behavior of Cu-26Zn-5Al alloy processed by accumulative roll bonding and heat treatment*, Journal of Alloys and Compounds, 924 (2022) 166574.
https://doi.org/10.1016/j.jallcom.2022.166574

[6] F. Iacoviello, V. Di Cocco, S. Natali, A. Brotzu, Grain size and loading conditions influence on fatigue crack propagation in a Cu-Zn-Al shape memory alloy, Int. J. Fatigue 115 (2018) 27–34, https://doi.org/10.1016/j.ijfatigue.2018.06.039

[7] A.O. Moghaddam, M. Ketabchi, R. Bahrami, Kinetic grain growth, shape memory and corrosion behavior of two Cu-based shape memory alloys after thermomechanical treatment, Trans. Nonferrous Met. Soc. China 23 (2013) 2896–2904, https://doi.org/10.1016/S1003-6326(13)62812-5

[8] V. Asanović, K. Delijić, N. Jauković, A study of transformations of β-phase in Cu-Zn-Al shape memory alloys, Scr. Mater. 58 (2008) 599–601, https://doi.org/10. 1016/j.scriptamat.2007.11.033

[9] L.G. Bujoreanu, N.M. Lohan, B. Pricop, N. Cimpoeşu, Thermal Memory Degradation in a Cu-Zn-Al Shape Memory Alloy During Thermal Cycling with Free Air Cooling, J. Mater. Eng. Perform. 20 (2011) 468–475, https://doi.org/10. 1007/s11665-010-9702-5

[10] C. Tudora, M. Abrudeanu, S. Stanciu, D. Anghel, G.A. Plaiasu, V. Rizea, I. Stirbu, N. Cimpoesu, B.A. Prisacariu, Heating to thermal shock of Cu-based {SMA} using a solar concentrator, {IOP} Conf. Ser. Mater. Sci. Eng. 444 (2018) 32014, https:// doi.org/10.1088/1757-899x/444/3/032014

[11] J. Mohd Jani, M. Leary, A. Subic, M.A. Gibson, A review of shape memory alloy research, applications and opportunities, Mater. Des. 56 (2014) 1078–1113, https://doi.org/10.1016/j.matdes.2013.11.084

[12] K.K. Alaneme, E.A. Okotete, N. Maledi, Phase characterisation and mechanical behaviour of Fe–B modified Cu–Zn–Al shape memory alloys, J. Mater. Res. Technol. 6 (2017) 136–146, https://doi.org/10.1016/j.jmrt.2016.10.003

This is the accepted manuscript (postprint) of the following article:
N. Negahdari, M. Alizadeh, S. Pashangeh, E. Salahinejad, *Structure and corrosion behavior of Cu-26Zn-5Al alloy processed by accumulative roll bonding and heat treatment*, Journal of Alloys and Compounds, 924 (2022) 166574.
https://doi.org/10.1016/j.jallcom.2022.166574

[13] R. Agnihotri, S. Bhardwaj, Synthesis and Characterization of CuZnAl Based Shape Memory Alloys and to Optimize Behavior on Different Properties by Varying Weight Percentage, Int. J. Mater. Sci. Eng. Synth. 4 (2016) 229–234, https://doi.org/10.17706/ijmse.2016.4.4.229-234

[14] A. Agrawal, R. Dube, Methods of fabricating Cu-Al-Ni shape memory alloys, J. Alloy. Compd. 750 (2018) 235–247.

[15] M. Alizadeh, M.K. Dashtestaninejad, Fabrication of manganese-aluminum bronze as a shape memory alloy by accumulative roll bonding process, Mater. Des. (2016) 263–270 https://doi.org/DOI:101016/jmatdes201608074.

[16] J.S. Lee, C.M. Wayman, Grain refinement of Cu-Zn-Al shape memory alloys, Metallography 19 (1986) 401–419, https://doi.org/10.1016/0026-0800(86) 90074-1

[17] D. Ćorić, I. Žmak, Influence of ausforming treatment on super elasticity of Cu-Zn- Al shape memory alloy for seismic energy dissipaters, Buildings 11 (2021) 1–15, https://doi.org/10.3390/buildings11010022

[18] S.K. Wu, W.J. Chan, S.H. Chang, Damping characteristics of inherent and intrinsic internal friction of Cu-Zn-Al shape memory alloys, Met. (Basel) 7 (2017) 1–10, https://doi.org/10.3390/met7100397

[19] N. Si, K. Sun, S. Sun, H. Liu, Damping performance of Cu-Zn-Al shape memory alloys in engineering structures, J. Cent. South Univ. Technol. 11 (2004) 246–251, https://doi.org/10.1007/s11771-004-0050-1

[20] B. De Filippo, A. Brotzu, S. Natali, Corrosion behavior of Cu-Zn-Al shape memory alloy in controlled environments, Environments 020013 (2020) 5–12.

This is the accepted manuscript (postprint) of the following article:
N. Negahdari, M. Alizadeh, S. Pashangeh, E. Salahinejad, *Structure and corrosion behavior of Cu-26Zn-5Al alloy processed by accumulative roll bonding and heat treatment*, Journal of Alloys and Compounds, 924 (2022) 166574.
https://doi.org/10.1016/j.jallcom.2022.166574

[21] M. Alizadeh, M. Avazzadeh, Evaluation of Cu-26Zn-5Al shape memory alloy fabricated by accumulative roll bonding process, Mater. Sci. Eng. A 757 (2019) 88–94, https://doi.org/10.1016/j.msea.2019.04.092

[22] M. Alizadeh, M.K. Dashtestaninejad, Development of Cu-matrix, Al/Mn-reinforced, multilayered composites by accumulative roll bonding (ARB, J. Alloy. Compd. 732 (2018) 674–682, https://doi.org/10.1016/j.jallcom.2017.10.211

[23] M. Stern, A.L. Geaby, Electrochemical polarization, J. Electrochem. Soc. 104 (1957) 56, https://doi.org/10.1149/1.2428496

[24] E. Aldirmaz, H. Celik, I. Aksoy, SEM and X-ray diffraction studies on microstructures in Cu-26.04%Zn-4.01%Al alloy, Acta Phys. Pol. A. 124 (2013) 87–89, https://doi.org/10.12693/APhysPolA.124.87

[25] Z. Stošić, D. Manasijević, L. Balanović, T. Holjevac-Grgurić, U. Stamenković, M. Premović, D. Minić, M. Gorgievski, R. Todorović, Effects of composition and thermal treatment of Cu-Al-Zn alloys with low content of Al on their shape- memory properties, Mater. Res. 20 (2017) 1425–1431, https://doi.org/10.1590/ 1980-5373-MR-2017-0153

[26] R. Zengin, N. Kayal, Struct. Morphol. Investig. Shape Mem. CuZnAl Alloy. 118 (2010).

[27] E. Aldirmaz, H. Celik, I. Aksoy, SEM and X-ray diffraction studies on microstructures in Cu-26.04%Zn-4.01%Al Alloy, Acta Phys. Pol. A. 124 (2013) 87–89, https://doi.org/10.12693/APhysPolA.124.87

[28] S.S. Leu, C.T. Hu, The aging effect on Cu−Zn−Al shape memory alloys with low contents of aluminum, Metall. Trans. A 22 (1991) 25–33, https://doi.org/10.1007/ BF03350946

This is the accepted manuscript (postprint) of the following article:
N. Negahdari, M. Alizadeh, S. Pashangeh, E. Salahinejad, *Structure and corrosion behavior of Cu-26Zn-5Al alloy processed by accumulative roll bonding and heat treatment*, Journal of Alloys and Compounds, 924 (2022) 166574.
https://doi.org/10.1016/j.jallcom.2022.166574

[29] A. Cuniberti, R. Romero, M. Stipcich, Stabilization kinetics and defects retained by quenching in 18R Cu–Zn–Al martensite, J. Alloy. Compd. 472 (2009) 162–165, https://doi.org/10.1016/j.jallcom.2008.05.005

[30] F. de Castro Bubani, M. Sade, F. Lovey, Improvements in the mechanical properties of the 18R↔6R high-hysteresis martensitic transformation by nanoprecipitates in CuZnAl alloys, Mater. Sci. Eng. A 543 (2012) 88–95, https://doi.org/10. 1016/j.msea.2012.02.051

[31] P.R. Roberge, Corrosion Engineering: Principles and Practice, McGraw-Hill, New York, 2008.

[32] H. Farajzadeh Dehkordi, M.R. Toroghinejad, K. Raeissi, Fabrication of Al/Al_2O_3/TiC hybrid composite by anodizing and accumulative roll bonding processes and investigation of its microstructure and mechanical properties, Mater. Sci. Eng. A 585 (2013) 460–467, https://doi.org/10.1016/j.msea.2013.07.075

[33] Z. Li, Microstructure evolution and corrosion behavior of Al-Si/Al-Mn composites un salt spray, Mater. Technol. 56 (2022) 139–147, https://doi.org/10.17222/mit. 2022.354

[34] S.N. Saud, E. Hamzah, T. Abubakar, S. Farahany, Structure-property relationship of Cu-Al-Ni-Fe shape memory alloys in different quenching media, J. Mater. Eng. Perform. 23 (2014) 255–261, https://doi.org/10.1007/s11665-013-0759-9

[35] S.N. Saud, E. Hamzah, T. Abubakar, H.R. Bakhsheshi-rad, Correlation of microstructural and corrosion characteristics of quaternary shape memory alloys Cu–Al–Ni–X (X]Mn or Ti, Trans. Nonferrous Met. Soc. China 25 (2015) 1158–1170, https://doi.org/10.1016/S1003-6326(15)63711-6